iScience

CellPress
OPEN ACCESS

Article

Harvesting water surface energy: self-jumping nanostructured hydrophobic metals

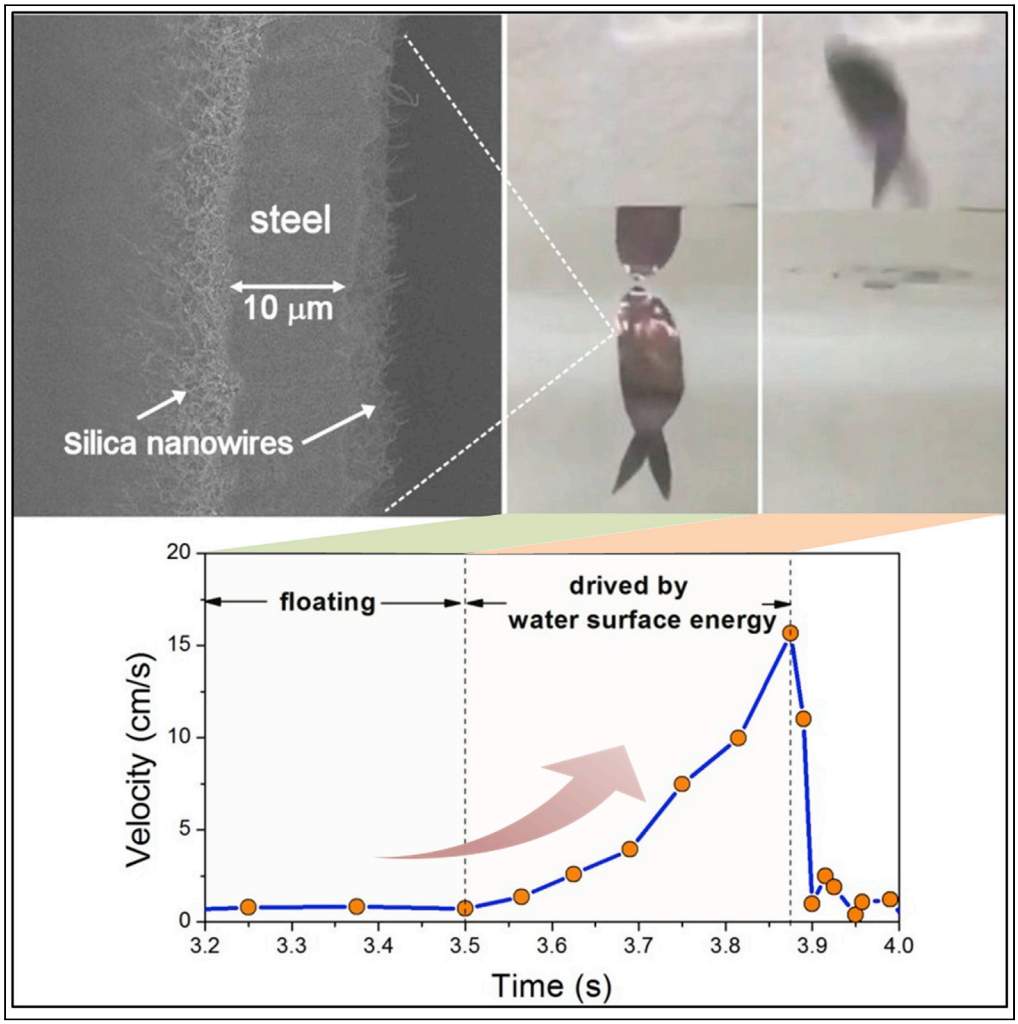

Jing Yuan Tsai, Guan Fu Huang, Jiann Shieh, Chin Chi Hsu, Kostya (Ken) Ostrikov

jshieh@nuu.edu.tw

Highlights

Thin metals with nanostructured hydrophobic surface become unsinkable

Surface energy conversion to eject metal from water

Twenty-fold speed boost of metal foil by water surface energy

Tsai et al., iScience *24*, 102746
July 23, 2021
https://doi.org/10.1016/j.isci.2021.102746

iScience

CellPress
OPEN ACCESS

Article

Harvesting water surface energy: self-jumping nanostructured hydrophobic metals

Jing Yuan Tsai,[1] Guan Fu Huang,[1] Jiann Shieh,[1,4,*] Chin Chi Hsu,[2] and Kostya (Ken) Ostrikov[3]

SUMMARY

Water in motion is a significant energy source worldwide, but the surface energy of water is rarely utilized as a power source. In this study, we made metals unsinkable and able to jump out of the water by harvesting the water surface energy. This effect is attributed to the enhanced floating ability of the nanostructures on copper and stainless steel foil surfaces. Sufficiently thin hydrophobic metals can slowly float underwater through air trapping at the surface and then rapidly leap out of the water on contact with the water-air interface. The mechanism is related to the surface energy of the water, which contributes to the 15 mg metals with a power of 0.49 μW experiencing rapid changes in velocity and acceleration at the interface. The conversion of surface energy to eject nanostructured hydrophobic materials from the liquid surface may lead to new solid-liquid separation techniques.

INTRODUCTION

Many organisms in nature can leap out of the water if they have sufficient inertia to overcome gravity and the surface tension of the water (Chang et al., 2019). However, for tiny organisms such as plankton, surface tension is the main obstacle to leaping; hence, their initial velocity must be sufficiently high to break through the water surface (Kim et al., 2015). Such leaps require organisms to generate momentum. Unlike organisms, common inorganic materials such as metals cannot generate self-kinetic energy and momentum to overcome gravity and, thus, cannot leap out of a water surface without external forces. The water-air surface tension also restricts the water exits of artificial robots (Feldmann et al., 2020). The ability of the metal to sink or float depends on its density, shape, and amount of water it displaces. Unshaped metals (e.g., plates) tend to sink when placed in water, owing to their high density. Deliberately shaped metals (e.g., boats) can float if the buoyancy generated by the displaced water exceeds their self-weight. Thus, metals are shaped to displace more water and float heavier or loaded boats. This ability is further improved with superhydrophobic surfaces exhibiting extreme water-repellent behavior and has been harnessed in many applications (Lafuma and Quéré, 2003; Liu et al., 2017). With nanoscale roughness and low surface energy, some air bubbles can be trapped at the water-metal interface to repel water (Arzt et al., 2021; Shieh et al., 2010). The attached air bubbles or layers can enhance the floating ability, as was applied to construct boats using superhydrophobic copper grids (Pan and Wang, 2009). The superhydrophobic surface provides an air layer to replace larger volumes of water for higher buoyancy (Guo et al., 2015). However, similar to conventional boats, the ability to rise to the surface is lost upon sinking (Yong et al., 2014). The metal shell of the sunken boat (with the air layer around it) displaces significantly less water than the shape of the boat floating on the surface (Hwang et al., 2017; Vella, 2015).

Recently, it has been reported that metal assemblies with superhydrophobic surfaces can be unsinkable, that is, after releasing the load, the assembly can float back to the water surface by trapping air inside the assembly (Zhan et al., 2019). However, without air trapping in the assembly, the superhydrophobic metal will permanently sink when the downward gravity exceeds the buoyancy from the air-loading capacity of the metal. Only a few studies have attempted to produce unshaped unsinkable metal plates; the limited success is attributed to the insufficient buoyancy impacted by the superhydrophobic surface.

In this study, these challenges were addressed by growing silica nanowires on sufficiently thin metal foils. We observed that these nanowires enabled metals to be unsinkable and to also be energized by the water

[1]Department of Materials Science and Engineering, National United University, Miaoli 36063, Taiwan

[2]Department of Mechanical Engineering, National United University, Miaoli 36063, Taiwan

[3]School of Chemistry and Physics and Centre for Materials Science, Queensland University of Technology, Brisbane, QLD 4000, Australia

[4]Lead contact

*Correspondence: jshieh@nuu.edu.tw

https://doi.org/10.1016/j.isci.2021.102746

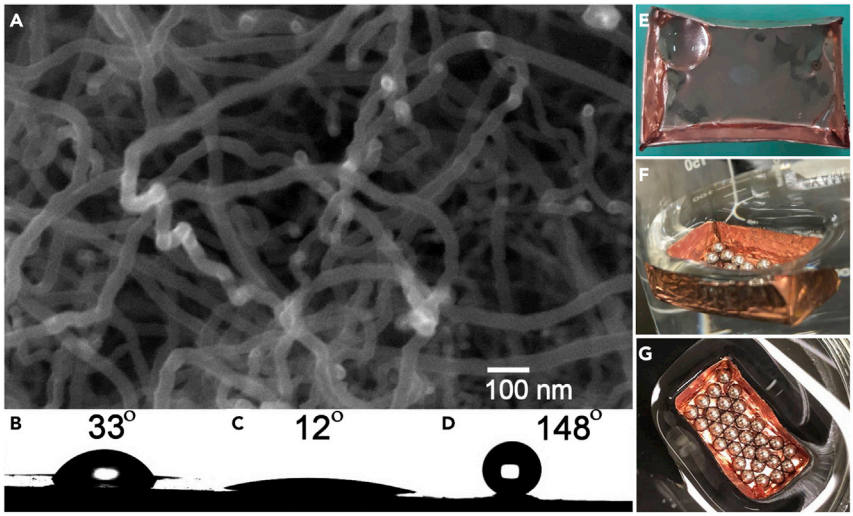

Figure 1. Silica nanowires grown on copper foil to provide hydrophilic and hydrophobic properties

(A) SEM image of silica nanowires grown on copper foil.

(B–D) Optical micrographs of water droplets at bare, hydrophilic, and hydrophobic copper foils, respectively.

(E) Photograph of water droplet sitting inside hydrophobic copper miniboat.

(F and G) Photographs of copper miniboat filled with stainless balls for loading measurement.

surface. Water is an abundant source of energy and traditional hydropower, and advancements have been made in water energy extraction by controlling the interactions between water molecules and nanostructured materials that help harvest hydrovoltaic (Xu et al., 2020; Yin et al., 2020) and triboelectric energy (Lia et al., 2020; Ma et al., 2019; Wang and Yang, 2019; Zhao et al., 2016). However, only a few studies have been conducted to explore the conversion of the water surface energy. Here we observed that the water surface energy could be converted into the kinetic power of metals for self-jumping. We first fabricated a copper miniboat to evaluate the effects of a hydrophobic surface that provides additional buoyancy to its floating capacity. We showed that, when the additional buoyancy is larger than the weight of the miniboat, the miniboat may be unsinkable. Similar unsinkable behavior was achieved for a thin stainless steel foil. Unprecedentedly, this thin metal foil can leap out of the water on contact with the water surface. Our results indicated that the water tension-powered sudden change in the velocity of the leap out of the water could explain this behavior.

RESULTS

Because of the good plasticity and high melting point of copper, above the process temperature (830°C), we prepared copper miniboats by folding the copper foil into different sizes to evaluate the effect of hydrophobic surfaces on the floating capacity. The surface morphology of the nanowires was characterized through scanning electron microscopy (SEM, Figure 1A). The randomly oriented nanowires had an average diameter of ~30 nm and a high aspect ratio. Detailed characterization of the silica nanowires is reported in our previous papers (Lee et al., 2019; Tsai and Shieh, 2019). The method of growing the silica nanowires based on the assistance of a metal catalyst through an active oxidation mechanism (Shalav et al., 2011) applies to various substrates, such as silicon, glass, ceramic, and metal substrates. The water contact angle of the bare copper foil was approximately 33° (Figure 1B). After the growth of the silica nanowires, the contact angle decreased to 12° (Figure 1C), owing to the surface roughness of the nanowires. Because silica has the advantage of easy covalent grafting to low-surface-energy silane with fluorinated backbones, such as tridecafluoro-(1,1,2,2)-tetrahydrooctyl-trichlorosilane ($C_8H_4Cl_3F_{13}Si$, F_{13}-TCS) (Beck et al., 2002), the surface can be converted from hydrophilic to hydrophobic. After coating the F_{13}-TCS silane monolayer, the water contact angle increased to 148° (Figure 1D). A water droplet could roll around inside the copper miniboat and does not spread out even when in contact with the interior (Figure 1E), indicating that all miniboat surfaces were highly hydrophobic. We then assessed the loading capacity of the miniboat by placing stainless steel balls inside the miniboat and adding water to determine the maximum weight of the miniboat that could remain buoyant before sinking (Figures 1F and 1G). The water surface bent at the upper edge of the boat because of hydrophobicity to provide surface tension to support the

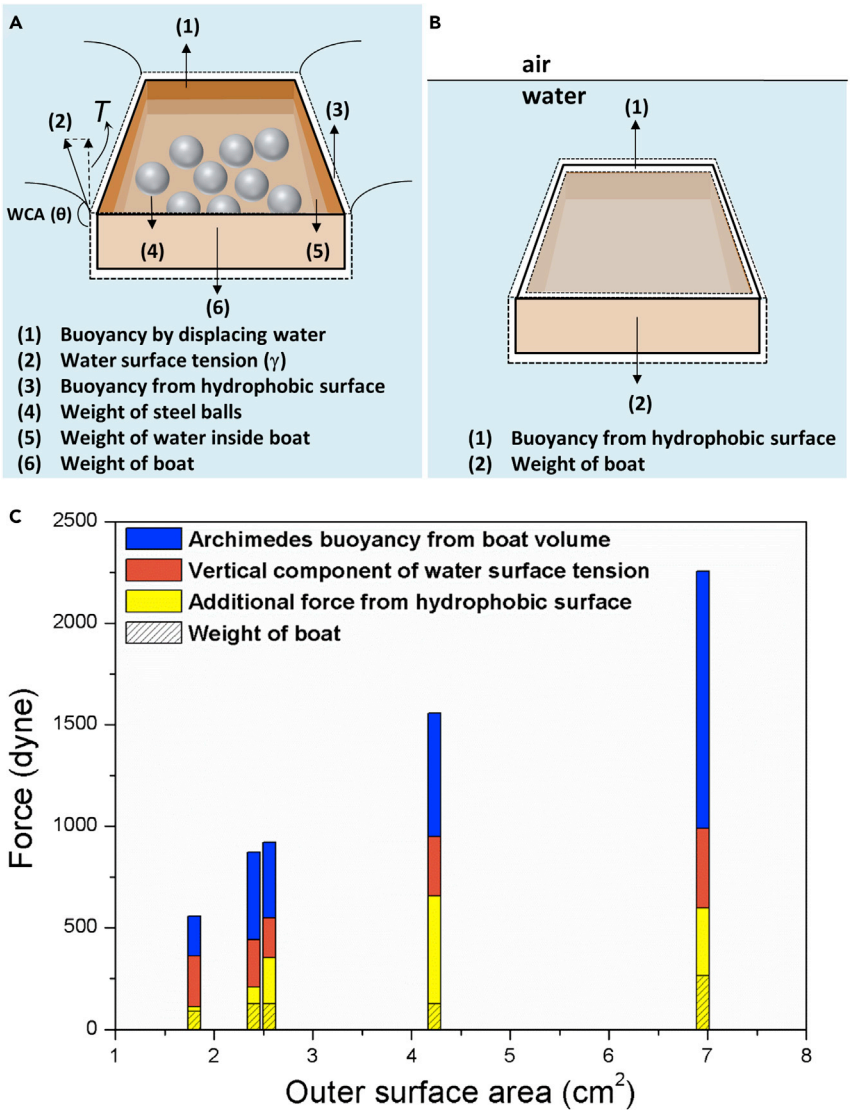

Figure 2. Hydrophobic nanowires on Cu surface to provide additional buoyancy

(A) Schematic of forces on floating miniboat.

(B) Schematic of forces on submerged miniboat.

(C) Measured buoyancy of copper miniboats with (total) and without (blue bars) hydrophobic nanowires as function of outer surface area of boat. The water surface tension (orange bars) around the upper edge of the boat was calculated, and the difference between the total force and the sum of orange and blue bars was the contribution from the air layer on the hydrophobic surface (yellow bars). The miniboat weights (dash bars) are also presented for comparison and are lower than the yellow bars at each surface area.

boat (Figure 2A). In addition, the air layer on the outer surface and the volume displaced by the boat also contributed to the buoyancy force, opposed to the total weight force from the boat, steel balls, and water added to the boat. When the boat submerged in water, only the additional buoyancy from the hydrophobic surface compensated for gravity (Figure 2B). We measured the buoyancy as a function of the outer surface area of the boat (Figure 2C). The boat buoyancy without nanowires was evaluated based on the weight of the water that the boat could carry, which was equal to the displaced water volume. The contribution of the bent water surface on floating was evaluated based on the vertical components of the water surface tension on the boat, derived as follows:

$$T = \gamma|\cos\theta|l \qquad \text{(Equation 1)}$$

where T is the upward force from the vertical component of the water surface tension, γ is the surface tension of the water, θ is the water contact angle, and l is the perimeter of the upper edge of the miniboat. The results showed that the measured buoyancy of the miniboat after the hydrophobic treatment was significantly higher than that of the bare miniboat. The difference in buoyancy was attributed to the air layer formed on the hydrophobic surface and the surface tension of the water in contact with the boat. The submerged hydrophobic miniboat had a bright mirror appearance (Figure S1), indicating that an air layer existed on the surface (Kavalenka et al., 2015; Liu et al., 2016; McHale et al., 2010; Röhrig et al., 2014). The weights of the miniboats (Figure 2C) were less than the additional buoyancy provided by the air layer at each specified outer surface area, indicating that only the hydrophobic surface may help the boat become unsinkable.

Unlike in previous research on superhydrophobic metal plates (Zhan et al., 2019), our boat floated back to the water surface even when pressed into water (Video S1). In addition, when the miniboat was unfolded, the unshaped metal foil remained unsinkable, even though the amount of water replaced by the metal volume was significantly lower than that of the floating miniboat (Video S2). For both the submerged and unfolded samples, the floating ability was attributed to the hydrophobic surface because the Archimedes' buoyancy from shaped boat was absent. For a specific surface area, the above results showed that buoyancy could be increased by decreasing the thickness of the sample. By thinning the foil to increase the surface area-to-weight ratio, the metal is made unsinkable, provided that the additional buoyancy exceeded the weight of the metal.

Compared with copper, the plasticity of steel is unsuitable for folding, but its stiffness enables the surface to remain flat, which is favorable for producing an unsinkable metal plate. Consequently, we grew silica nanowires from 304 stainless steel foils with a 0.01 mm thickness. Figure 3A shows a SEM image of the nanowires grown on steel. After F_{13}-TCS coating, the water contact angle of the metal foils increased from ~17° to ~144° (inset of Figure 3A), and the steel foils exhibited nonwetting behavior as they were immersed in water (Video S3). The cross-sectional SEM images (Figures 3B and 3C) demonstrated that the nanowires were uniformly distributed on the foil surface with a thickness of ~3.5 μm.

This hydrophobic thin steel foil exhibited an unsinkable behavior. Figure 3D shows a snapshot of the floating process from Video S4 (the complete record is shown in Figure S2). We recorded the position of the sample center over time (Figure 3E). When the hydrophobic steel foil was released underwater, it began to float slowly and then started jumping up when it touched the water surface. In addition to the contribution by the additional buoyancy, the lower drag that accompanied hydrophobicity could assist the metal in floating. The velocity derived from the position increased as the foil left the water surface and then decreased when subjected to gravity (Figure 3F). The acceleration obtained from the velocity diagrams also demonstrated that the water surface generated a force that pushed the foil upward (Figure 3G). This evidence suggested that the surface tension of water played a significant role in the jump. We also prepared a fish-shaped sample to compare with the jumping of dolphins (Figures 3H and Video S5) and found that the inorganic material was capable of self-jumping by nanoscale surface engineering.

As we dipped the foil into the water and pulled it up, we observed that a convex shape of the water surface was formed on the foil (Figure 4A), revealing that the surface tension could facilitate the metal jump. Figures 4B–4D show a schematic of the steel foil floating out of the water from the principal directions in space. Bormashenko demonstrated that the surface tension dominates the floating behavior of elongated bodies when the characteristic length is shorter than the capillary length of water (Bormashenko, 2016). Because the steel foil thickness (0.01 mm) was significantly smaller than the capillary length of the water (2.71 mm), the vertical component of the capillary force was critical for the floating and proportional to the three-phase (air-water-solid) line perimeter (Bormashenko, 2016) when the steel foil protruded from the water surface (Figure 4C). Thus, as the foil started to penetrate the water surface, the three-phase line and the corresponding capillary force increased gradually (Figure 4D), forcing the foil to leap out of the water surface. As the foil left the water surface, gravity dominated the fall of the foil in the absence of buoyancy and capillary forces.

The highly hydrophobic surface was essential for the unsinkable properties. Based on our comparison of the pristine, silane-coated, and hydrophilic and hydrophobic nanowire foils, only the hydrophobic nanowire sample exhibited unsinkable behavior (Video S6). The as-prepared hydrophilic nanowire sample

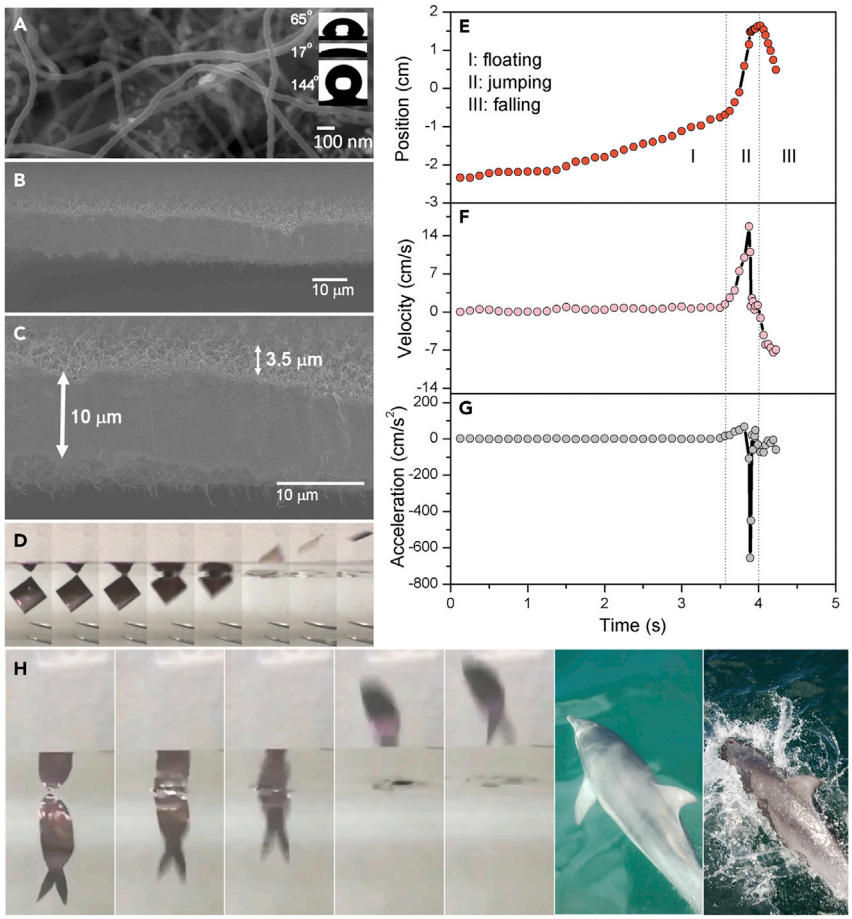

Figure 3. Hydrophobic nanowires to make the metal foil jump out of water

(A) Top-view SEM image of silica nanowires grown on stainless steel foil; the inset shows water droplets sitting on the bare (65°), hydrophilic (17°), and hydrophobic (144°) steel foils.

(B and C) Cross-sectional SEM images of silica nanowires grown on stainless steel foil.

(D–G) (D) Snapshot of stainless steel foil floating and self-jumping out of water. Time-dependent (E) position, (F) velocity, and (G) acceleration of stainless steel foils derived from snapshot shown in Figure S2.

(H) Unlike dolphins, sufficiently thin hydrophobic metal plates gainfully utilized surface tension to jump out of water without any external energy input.

sank immediately, indicating that the nanowires minimally contributed to the decrease in the effective density of the sample.

DISCUSSION

Our experimental study has shown that metals with a high surface area-to-weight ratio can float and even jump out from the water after growing silica nanowires and grafting low-energy molecules on their surface. In contrast to previous research, our study has shown that a copper miniboat can float back to the surface as it is submerged into water. Unprecedentedly, a stainless steel foil can self-jump out of the water surface and overcome gravity without the action of any external force. This difference may be related to the thickness of the metal foil. For example, Zhan et al. used an Al plate of 0.2 mm thickness to evaluate the floating ability (Zhan et al., 2019); this plate was significantly thicker than our stainless steel foil (0.01 mm). As we grew the silica nanowires on a 0.05-mm-thick foil, the submerged sample could not float back to the water surface (Video S7). We can evaluate the effective air layer thickness by comparing the densities of stainless steel (7.93 g/cm^3) and water (1 g/cm^3). The nanowires on the effective thickness of the air layer must be larger than 34 μm for a 10-μm-thick foil on both sides to make the metal float (Figure S3). The appearance of a silvery sheen from the immersed sample is shown in Figure S1, which provides evidence of an air layer

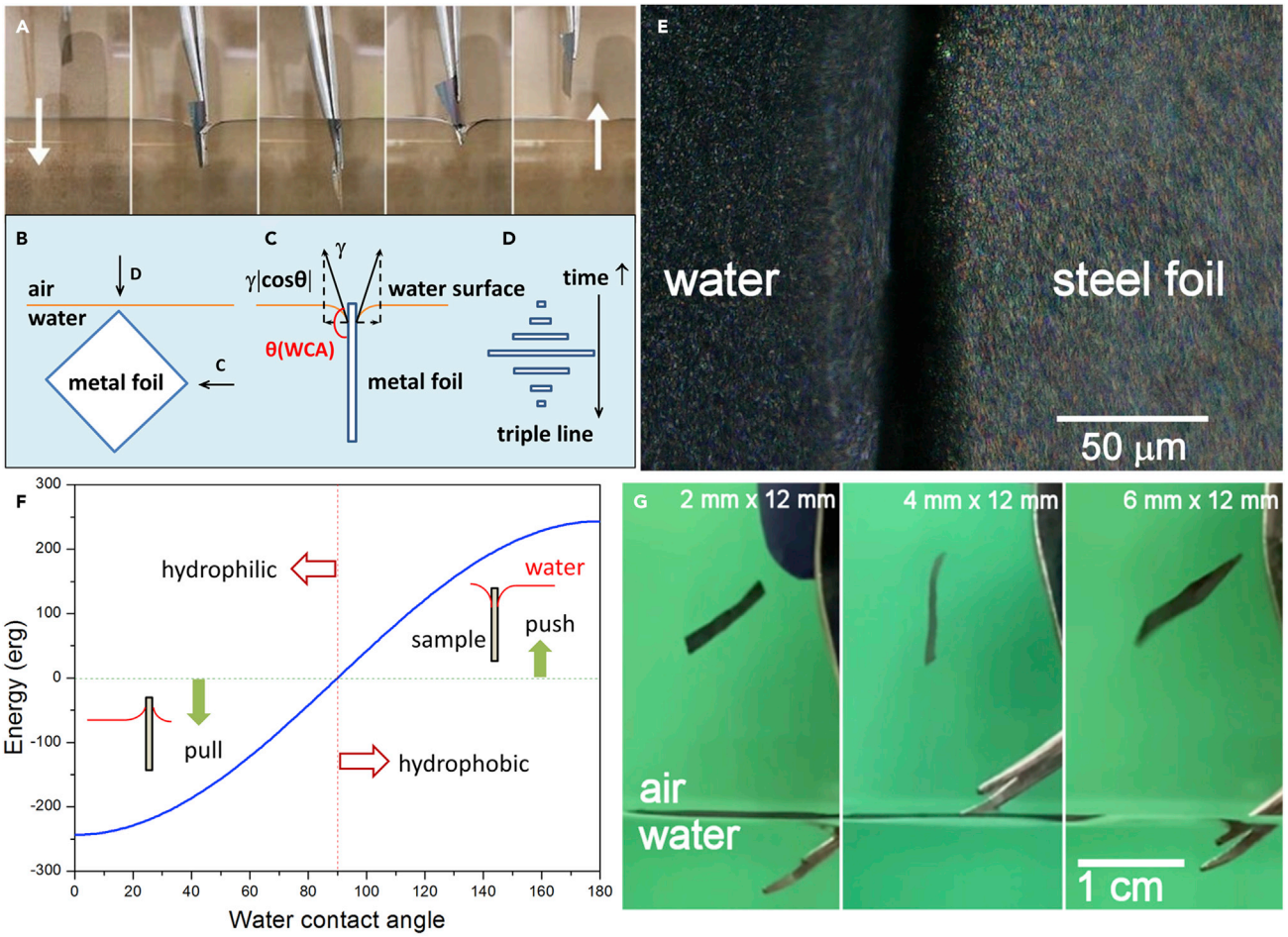

Figure 4. Bending water surface to drive the jumping of metal foils

(A) Photographs of the stainless steel foil immersed and pulled out of water. The superhydrophobic surface bends the water surface and provides a driving force for the foil to jump out of the water.

(B) Schematic of stainless steel foil immersed in water, where C and D represent directions of field of view in Figures 4C and 4D, respectively.

(C) Schematic of surface tension on stainless steel foil as it rises to the surface.

(D) Schematic of three-phase lines over time.

(E) Optical image of air layer between water and steel foil edge.

(F) Energy transferred to sample from water surface as function of water contact angle.

(G) Photographs of steel foil with different surface areas jumping to almost the same maximum height.

retained at the sample surface. Figure 4E shows an optical microscopic image of the air layer at the boundary between the steel foil and water, confirming water repulsion by the hydrophobic surface. Because the observed and calculated effective air layers were significantly thicker than the silica nanowire layer, we believe that the air trapped by hydrophobic nanowires enhanced buoyancy.

In different contexts, self-jumping phenomena have been observed in in-plane dropwise condensation (Boreyko and Chen, 2009; Wisdom et al., 2013) and spore discharge (Pringle et al., 2005). It has been suggested that the release of surface energy during coalescence contributes to the kinetic energy of the droplets. In contrast to the coalescence between droplets, we propose that the contact between the hydrophobic solid and the water surface also introduces an energy transition, which can be analyzed by integrating the water surface tension over the areas on both metal foil sides. Therefore, the work for the jump in the vertical direction by the water surface tension on the metal foil is expressed as follows:

$$\gamma|\cos\theta| \times A = 197\ erg \qquad \text{Equation 2}$$

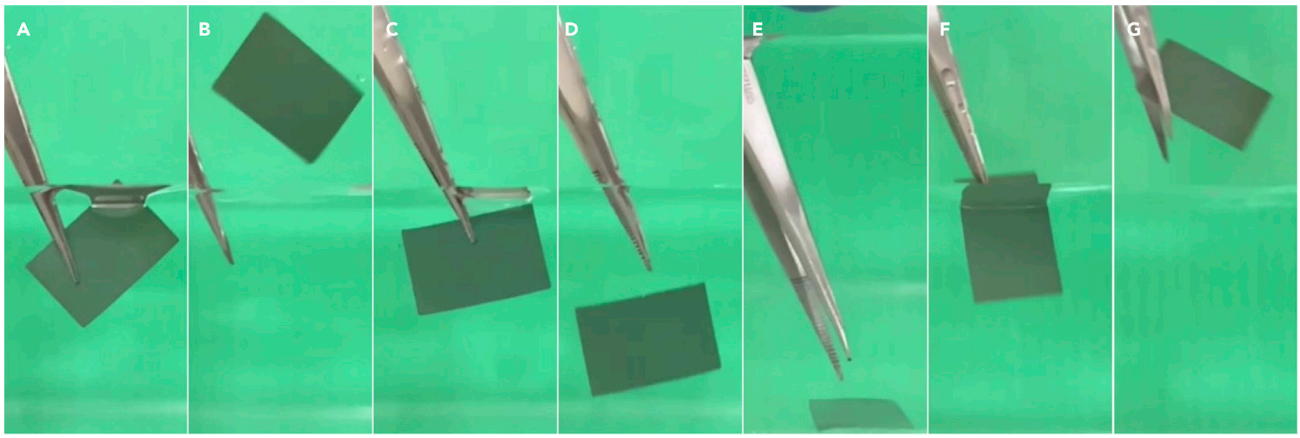

Figure 5. Air-water interface helps the hydrophobic stainless steel mesh jump out of the water

(A and B) Photographs of stainless steel mesh immersed and jumping by water surface.

(C and D) Mesh sinks underwater.

(E–G) Mesh jumps after picking up and touching water surface.

where γ is the surface tension of water (72 erg/cm^2), θ is the water contact angle on the hydrophobic steel foil (144°), and A is the total area of the metal foil (3.38 cm^2). In this case, this energy is sufficient for the metal foil to jump to a height h of 1.5 cm (the corresponding potential energy is mgh = 22 erg, where m is the foil mass, ≈15 mg). Based on the change in the velocity during jumping (0.375 s), we calculated the power generated from the water surface for this foil, which is ≈ 0.49 μW. The energy transferred to a 1.3 cm × 1.3 cm sample as a function of the water contact angle was also calculated (Figure 4F). For hydrophobic samples, the water surface plays the role of a lifesaver-floating device to pop it out, while the energy provided by the water surface increases with the contact angle. In contrast, for the hydrophilic samples, the water surface tension opposes their exit, similar to additional sinking weight. We further prepared samples of different sizes to investigate the contribution of the water surface energy to the jumping height of the metal foils. Figure 4G shows the maximum jumping heights of the samples with various surface areas from the screenshots in Video S8. Based on Equation (2), the work performed by the surface tension of water is proportional to the surface area; moreover, the weight of the foil is proportional to the surface area. Therefore, although larger surface areas enhanced the harvesting of more energy from the water surface, the metal foil jumped out of the water to reach the same height as a smaller metal foil because of its greater weight.

To gain further insight into the observed jumping phenomenon, we prepared a stainless steel mesh sample decorated with the same nanowires to evaluate the effect of the surface tension on the jumping (Figure 5 and Video S9). After nanowire growth and silane treatment, the metal mesh exhibited hydrophobicity at a water contact angle of 142° (Figure S4), and the shimmer appearance (Figure S1) suggested the existence of an underwater air layer on the mesh surface. When we partially immersed the sample in the water (Figure 5A), the mesh exhibited a similar jumping behavior (Figure 5B). However, the mesh sank downward when fully immersed in water (Figures 5C and 5D). As we picked the mesh up toward the water surface and released it after a complete stop (Figures 5E and 5F), we observed that the mesh also presented a similar self-jumping behavior (Figure 5G). This result reveals that the water surface tension dominates the leaping process even when the buoyancy is not sufficiently large to float the sample upward.

In summary, we developed an unsinkable metal plate that could leap out of the water as the plate was floated up and touched the water-air interface. The findings imply that the water-air interface may not always restrict the movement of immersed objects, as commonly believed. Instead, under the specific conditions investigated in this study, this interface can provide kinetic energy to hydrophobic objects by converting the surface energy from water and potentially other liquids. Our study can be extended to other hydrophobic materials, that is, it should not only be limited to metals. Future studies can open exciting opportunities for designing biomimetic intelligent systems and their diverse applications, including solid-liquid separation.

Limitations of the study

The hydrophobic surface facilitates the self-jumping of materials out of the water surface. When the weight of the thick metal foil exceeds the additional buoyancy provided by the hydrophobic surface, the jumping of the materials cannot occur.

STAR★METHODS

Detailed methods are provided in the online version of this paper and include the following:

- KEY RESOURCES TABLE
- RESOURCE AVAILABILITY
  - Lead contact
  - Materials availability
  - Data and code availability
- METHOD DETAILS
  - Materials
  - Growth of silica nanowires
  - Sample analysis

SUPPLEMENTAL INFORMATION

Supplemental information can be found online at https://doi.org/10.1016/j.isci.2021.102746.

ACKNOWLEDGMENTS

We thank Chiung Chih Hsu (Taiwan Semiconductor Research Institute) for the SEM analysis. This study was supported by the Ministry of Science and Technology, Taiwan (Grant No. MOST 109-2221-E-239-019 and MOST 109-2813-C-239-009-E).

AUTHOR CONTRIBUTIONS

Conceptualization, J.S.; methodology, J.S.; validation, J.Y.T. and G.F.H.; writing – original draft, J.S.; writing – review & editing, J.S., C.C.H., and K.O.; investigation, J.Y.T., G.F.H., J.S., C.C.H., and K.O.; funding acquisition, J.Y.T. and J.S.; resources, J.S.; supervision, J.S. and K.O.

DECLARATION OF INTERESTS

The authors declare no competing interests.

Received: March 5, 2021
Revised: May 17, 2021
Accepted: June 14, 2021
Published: July 23, 2021

REFERENCES

Arzt, E., Quan, H., McMeeking, R.M., and Hensel, R. (2021). Functional surface microstructures inspired by nature – from adhesion and wetting principles to sustainable new devices. Prog. Mater. Sci. *119*, 100778.

Beck, M., Graczyk, M., Maximov, I., Sarwe, E.-L., Ling, T.G.I., Keil, M., and Montelius, L. (2002). Improving stamps for 10 nm level wafer scale nanoimprint lithography. Microelectron. Eng. *61–62*, 441–448.

Boreyko, J.B., and Chen, C.H. (2009). Self-propelled dropwise condensate on superhydrophobic surfaces. Phys. Rev. Lett. *103*, 184501.

Bormashenko, E. (2016). Surface tension supported floating of heavy objects: Why elongated bodies float better? J. Colloid Interf. Sci. *463*, 8–12.

Chang, B., Myeong, J., Virot, E., Clanet, C., Kim, H.-Y., and Jung, S. (2019). Jumping dynamics of aquatic animals. J. R. Soc. Interf. *16*, 20190014.

Feldmann, D., Das, R., and Pinchasik, B. (2020). How can interfacial phenomena in nature inspire smaller robots. Adv. Mater. Inter. *8*, 2001300.

Guo, J., Yu, S., Li, J., and Guo, Z. (2015). Fabrication of functional superhydrophobic engineering materials via an extremely rapid and simple route. Chem. Commun. *51*, 6493–6495.

Hwang, G.B., Patir, A., Page, K., Lu, Y., Allan, E., and Parkin, I.P. (2017). Buoyancy increase and drag-reduction through a simple superhydrophobic coating. Nanoscale *9*, 7588–7594.

Kavalenka, M.N., Vüllers, F., Lischker, S., Zeiger, C., Hopf, A., Röhrig, M., Rapp, B.E., Worgull, M., and Hölscher, H. (2015). Bioinspired air-retaining nanofur for drag reduction. ACS Appl. Mater. Inter. *7*, 10651–10655.

Kim, S.J., Hasanyan, J., Gemmell, B.J., Lee, S., and Jung, S. (2015). Dynamic criteria of plankton jumping out of water. J. R. Soc. Interf. *12*, 20150582.

Lafuma, A., and Quéré, D. (2003). Superhydrophobic states. Nat. Mater. *2*, 457–460.

Lee, H.Y., Huang, B.W., Tsai, Y.C., and Shieh, J. (2019). Rapid, low-temperature growth of sub-10 nm silica nanowires through plasma

pretreatment for antireflection applications. ACS Appl. Nano Mater. *2*, 2836–2843.

Lia, G.Z., Wang, G.G., Cai, Y.W., Sun, N., Li, F., Zhou, H.L., Zhao, H.X., Zhang, X.N., Han, J.C., and Yang, Y. (2020). A high-performance transparent and flexible triboelectric nanogenerator based on hydrophobic composite films. Nano Energy *75*, 104918.

Liu, M., Wang, S., and Jiang, L. (2017). Nature-inspired superwettability systems. Nat. Rev. Mater. *2*, 17036.

Liu, Y., Zhang, K., Yao, W., Zhang, C., Han, Z., and Ren, L.A. (2016). Facile electrodeposition process for the fabrication of superhydrophobic and superoleophilic copper mesh for efficient oil−water separation. Ind. Eng. Chem. Res. *55*, 2704–2712.

Ma, X., Wang, Y., Wu, H., Wang, Y., and Yang, Y. (2019). Efficient water scavenging by cooling superhydrophobic surfaces to obtain jumping water droplets from air. Sci. Rep. *9*, 13784.

McHale, G., Newton, M.I., and Shirtcliffe, N.J. (2010). Immersed superhydrophobic surfaces: gas exchange, slip and drag reduction properties. Soft Matter *6*, 714–719.

Pan, Q., and Wang, M. (2009). Miniature boats with striking loading capacity fabricated from superhydrophobic copper meshes. ACS Appl. Mat. Inter. *1*, 420–423.

Pringle, A., Patek, S.N., Fischer, M., Stolze, J., and Money, N.P. (2005). The captured launch of a ballistospore. Mycologia *97*, 866–871.

Röhrig, M., Mail, M., Schneider, M., Louvin, H., Hopf, A., Schimmel, T., Worgull, M., and Hölscher, H. (2014). Nanofur for biomimetic applications. Adv. Mater. Inter. *1*, 1300083.

Shalav, A., Kim, T., and Elliman, R.G. (2011). SiO(x) nanowires grown via the active oxidation of silicon. IEEE J. Sel. Top. Quan. Electron. *17*, 785–793.

Shieh, J., Hou, F.J., Chen, Y.C., Chen, H.M., Yang, S.P., Cheng, C.C., and Chen, H.L. (2010). Robust airlike superhydrophobic surfaces. Adv. Mater. *22*, 597–601.

Tsai, Y.C., and Shieh, J. (2019). Growing invisible silica nanowires on fused silica plates provides highly transparent and superwetting substrates. Appl. Surf. Sci. *479*, 619–625.

Vella, D. (2015). Floating versus sinking. Annu. Rev. Fluid Mech. *47*, 115–135.

Wang, Y., and Yang, Y. (2019). Superhydrophobic surfaces-based redox-induced electricity from water droplets for self-powered wearable electronics. Nano Energy *56*, 574–584.

Wisdom, K.M., Watson, J.A., Qu, X., Liu, F., Watson, G.S., and Chen, C.H. (2013). Self-cleaning of superhydrophobic surfaces by self-propelled jumping condensate. PNAS *110*, 7992–7997.

Xu, W., Zheng, H., Liu, Y., Zhou, X., Zhang, C., Song, Y., Deng, X., Leung, M., Yang, Z., Xu, R.X., et al. (2020). A droplet-based electricity generator with high instantaneous power density. Nature *578*, 392–396.

Yin, J., Zhou, J., Fang, S., and Guo, W. (2020). Hydrovoltaic energy on the way. Joule *4*, 1852–1855.

Yong, J., Yang, Q., Chen, F., Zhang, D., Du, G., Si, J., Yun, F., and Hou, X. (2014). A bioinspired planar superhydrophobic microboat. J. Micromech. Microeng. *24*, 035006.

Zhan, Z., ElKabbash, M., Cheng, J., Zhang, J., Singh, S., and Guo, C. (2019). Highly floatable superhydrophobic metallic assembly for aquatic applications. ACS Appl. Mater. Inter. *11*, 48512–48517.

Zhao, K.Y., Wang, Z.L., and Yang, Y. (2016). Self-powered wireless smart sensor node enabled by an ultrastable, highly efficient, and superhydrophobic-surface-based triboelectric nanogenerator. ACS Nano *10*, 9044–9052.

STAR★METHODS

KEY RESOURCES TABLE

REAGENT or RESOURCE	SOURCE	IDENTIFIER
Chemicals, peptides, and recombinant proteins		
Acetone	Echo Chemical Co., Ltd.	CAS#67-64-1
Ethanol	Echo Chemical Co., Ltd.	CAS#64-17-5
Propanol	Echo Chemical Co., Ltd.	CAS#67-63-0
n-Hexane	Fisher Chemical	CAS#110-54-3
Copper	Alfa Aesar	CAS#7440508
Steel	Homytech	http://homytech.com/
Silicon wafer	Summit-Tech	http://www.summit-tech.com.tw
Hydrogen	Oriental Union Chemical Corp.	CAS#1333-74-0
Argon	Oriental Union Chemical Corp.	CAS#7440-37-1
Software and algorithms		
Origin 2018	Origin Lab	https://www.originlab.com/origin
PaintShop Pro 2019	Corel	https://www.paintshoppro.com/tw/
Video Maker	Microsoft	https://support.microsoft.com/
Other		
Synergy	Merck Millipore	https://www.merckmillipore.com/TW/zh/product/
Ultrasonic cleaners	Elma	https://www.elma-ultrasonic.com
Sputter coater	SPI Supplies	https://www.2spi.com/category/coaters/
Furnace CVD	Kao Duen	http://www.kaoduen.com.tw/product.php?lang = tw&tb = 1&cid = 69
Contact angle analyzer	Surface Electro Optics (Phoenix MT)	https://www.amtech.com.tw/product.html
Scanning electron microscope	JEOL (JSM-6700F; JSM-6500F)	http://www.jiedong.com.tw/products3.php?sub = 2
Optical microscope	Keyence (VHX-6000)	https://www.keyence.com/landing/microscope/digital_microscope_vhx6000.jsp

RESOURCE AVAILABILITY

Lead contact

Further information and requests for resources should be directed to and will be fulfilled by the lead contact, Jiann Shieh (jshieh@nuu.edu.tw).

Materials availability

New unique reagents were not generated in this study.

Data and code availability

Datasets were not generated in this study.

METHOD DETAILS

Materials

Silicon wafers were purchased from Summit-Tech. Copper and steel were obtained from Alfa Aesar and Homytech, respectively. F13-TCS were purchased from Uni-Onward. Acetone, ethanol, and propanol were purchased from Echo Chemical Co., Ltd. Hexane was purchased from Fisher Chemical. Deionized

water was prepared using a Milli-Q system (Millipore, USA). Hydrogen and argon gases were purchased from the Oriental Union Chemical Corp. All chemicals were used without further modification.

Growth of silica nanowires

Hydrophobic metals, including Cu and stainless steel decorated with silica nanowires, were grown through active oxidation. We first deposited Pt films as a catalyst on both the silicon wafers and metals through sputtering (SEM coater, SPI Supplies). The samples were ultrasonically cleaned with acetone, DI water, and isopropanol for 9 min before Pt deposition. The silicon wafers and samples were stacked layer by layer and separated using quartz spacers at a spacing of 5 mm in a high-temperature furnace. For the metal foils, hydrogen and argon gases were used as reaction gases at flow rates of 70 and 40 sccm, respectively. For the stainless steel mesh, we adopted an H2/Ar flow of 150/25 sccm to elongate the nanowires. The temperature was set to 830°C for a heating duration of 30 min, and the working pressure during the process was maintained at 5 Torr. This method provides a facile approach of growing nanowires from metals in which SiO vapor is transported from a silicon wafer, and the dewetting Pt reduces the growth temperature through a vapor–liquid–solid mechanism. The surface of the as-prepared metal was hydrophilic. We transferred the surface from hydrophilic to hydrophobic states through vapor deposition of F13-TCS silane because silica provided −OH groups to anchor low-energy silane molecules. The monolayer could be formed by bonding to the silica surface at 210°C for 2 hr after washing off the excess F13-TCS with n-hexane.

Sample analysis

The morphologies of the silica nanowires were examined through field-emission SEM (6500F and 6700F, JEOL). Carbon coatings were deposited before SEM analysis to increase the electrical conductivity for better resolution. The air layer was observed using an optical microscope (VHX-6000, Keyence). The wetting behavior of the metals was evaluated using a contact-angle goniometer (Phoenix MT) with deionized water droplets, and the result for each sample was obtained using more than three values. The volume of the water droplet for measurement was ~7 μL, and the contact angle was calculated using the tangent line method.